

# 1. Nuclei at very elongated shapes\*

## 1.1. Superdeformation: a brief survey

Long cascades of equally spaced  $\gamma$ -rays were initially observed in  $^{132}\text{Ce}$  [12] and  $^{152}\text{Dy}$  [13] using the TESSA family of spectrometers at Daresbury. The close energy spacing of these transitions implied a larger moment of inertia than the low-spin ground-state bands and was interpreted in terms of the rotation of a superdeformed nuclear shape based on a secondary minimum in the nuclear potential energy surface at large deformation. These very elongated superdeformed shapes are stabilised by fast collective rotation and thus can be produced experimentally in fusion-evaporation reactions only at high spin and with very small cross sections (at most a few percent of the fusion-evaporation reaction channel). To observe them it is absolutely indispensable to have the largest possible  $\gamma$ -ray detection efficiency and a very high resolving power.

Taking advantage of new developments in Ge detector technology, several generations of  $\gamma$ -ray spectrometers were built since this time (cf. Section 10) in order to investigate the phenomenon of superdeformation more precisely. With modern multi-detector Germanium arrays superdeformed rotational bands have been found in many new regions of the Segrè chart. With the EURO GAM spectrometer [3], for example, many yrast and excited superdeformed bands were found in the heavier nuclei ( $A \sim 130, 150, 190$ ) and more recently also around  $A \sim 170$ . An exhaustive review can be found in the “Table of Superdeformed Nuclear Bands and Fission Isomers” [14]. Several unexpected features were observed, like the identical superdeformed bands [15] and the “staggering effect” leading to  $\Delta I = 4$  structures [16], most of which are still not completely understood. Thanks to the increased sensitivity, discrete linking transitions between the second and the first well were established for several superdeformed nuclei (cf. Section 3) giving an unambiguous assignment of the spin and the parity of some superdeformed rotational bands [17].

---

\* Contribution by O. Stézowski and J. Wilson

In Figure 1.1 a representation of all nuclei is given, in which at least one superdeformed rotational band has been found. The data are taken from [14] and represent about seventy known superdeformed nuclei. In this figure, the new triaxial superdeformed bands (cf. Section 2) and also some light superdeformed nuclei are not yet indicated. Superdeformed nuclei of different mass regions often give access to different nuclear properties, i.e. single-particle vs. collective excitations and the disappearance of pairing at the highest spins or for extreme values of the rotational frequency. Superdeformation has been found to be present in many nuclei, but it is still a challenge to find new superdeformed bands

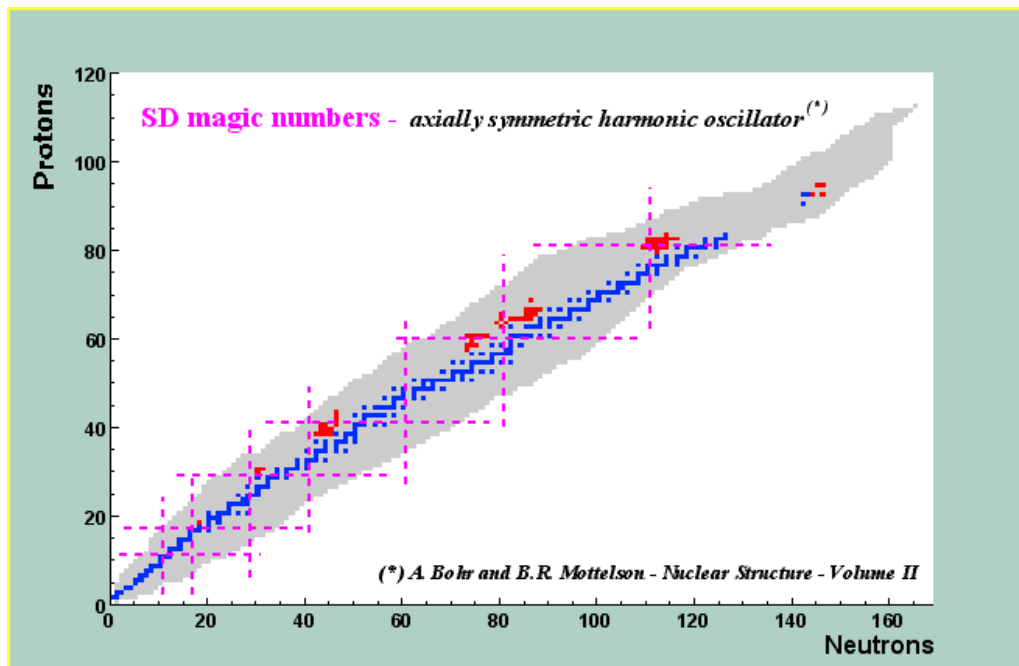


**Figure 1.1:** Superdeformation and the associated “magic” numbers (dashed lines) as given by Bohr and Mottelson [18] and compared to the actual mass regions where Superdeformation has been observed (shown in red). Stable nuclei are indicated in blue, while all nuclei known to exist are marked in grey.

either residing far from the known superdeformed magic numbers or involving deeply-bound orbitals, both effects leading to highly excited superdeformed states.

Using a rather simple (axially symmetric) anisotropic harmonic oscillator potential, Bohr and Mottelson [18] predicted, quite accurately, the superdeformed magic numbers. In fact, theory predicts even more mass regions than what has actually been observed (see dashed lines in Figure 1.1). However more advanced

theoretical calculations, often going beyond the mean-field approach, are needed in order to understand the structure of superdeformed nuclei in detail. These models have shown that the behaviour of the (dynamic) moment of inertia ( $\mathfrak{I}^{(2)}$ ) for superdeformed rotational bands, is generally governed by the number of intruder orbitals occupied (see, e.g. [19], for results based on the macroscopic-microscopic approach). In this way the configuration of most of the superdeformed bands has been interpreted as based on single-particle (or quasi-particle) excitations obtained in a pure axially symmetric quadrupole type mean field. This represents a reasonable first order approximation, but in some cases other degrees of freedom need to be taken into account for a realistic description of the second well. Thus, some experimental findings can only be interpreted by the occurrence of stable triaxial superdeformed minima (cf. Section 2) like, for instance, in the  $A\sim 170$  mass region, in  $^{154}\text{Er}$  [20] or in  $^{86}\text{Zr}$  [21]. In some cases, especially in the  $A\sim 190$  mass region, also indications for an octupole vibrational character of the excited superdeformed states were obtained.

With EUROBALL, a broad and extensive study of the second well has been realised and, in particular, single-particle or quasi-particle excitations, collective vibrational states and shape coexistence have been investigated. With its high resolving power, large efficiency and dedicated additional detectors (i.e. the INNER BALL calorimeter to measure the total gamma-ray sum energy and multiplicity) it has been possible to find many excited superdeformed bands populated with very small cross sections. In particular, the strongly deformed triaxial nuclei observed in the  $A\sim 170$  mass region have been thoroughly investigated (cf. Section 2). The high sensitivity of EUROBALL has also allowed known superdeformed rotational bands to be investigated in more detail. New information was also obtained for discrete linking transitions between the second and the first well (cf. Section 3).

The knowledge of these transitions is crucial to determine the spin, parity and excitation energy of superdeformed states. Magnetic and collective properties can be established by investigating transitions connecting different superdeformed rotational bands. In the following sections some of the main results that EUROBALL has brought concerning the phenomenon of superdeformation will be emphasised. A more exhaustive review on the influence of microscopic structures on the rotational motion of superdeformed nuclei can be found in [22].

## 1.2. New results related to superdeformed rotational bands

### Identical Bands

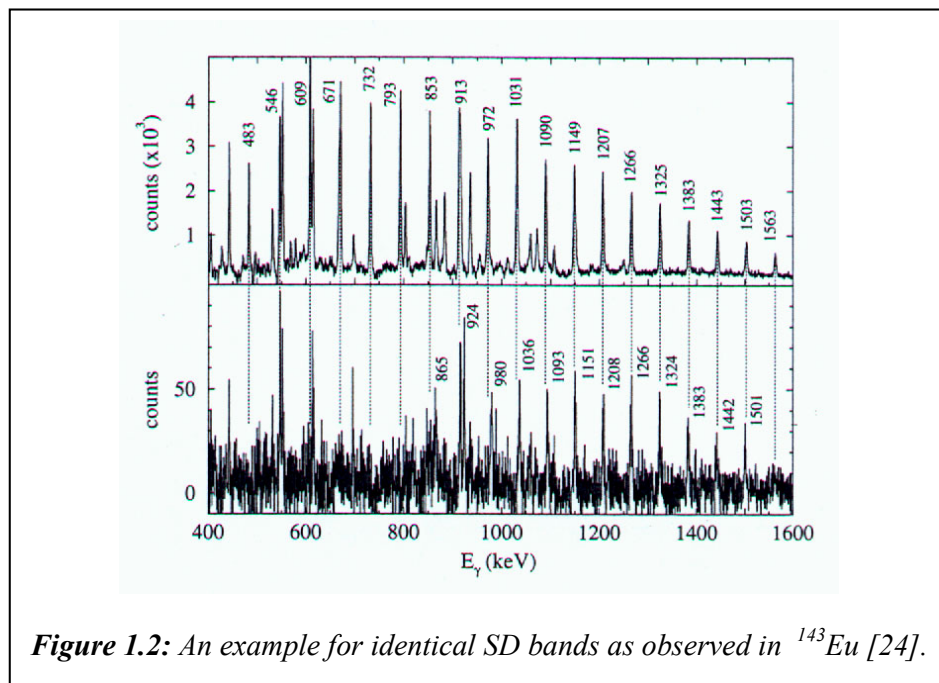


**Figure 1.2:** An example for identical SD bands as observed in  $^{143}\text{Eu}$  [24].

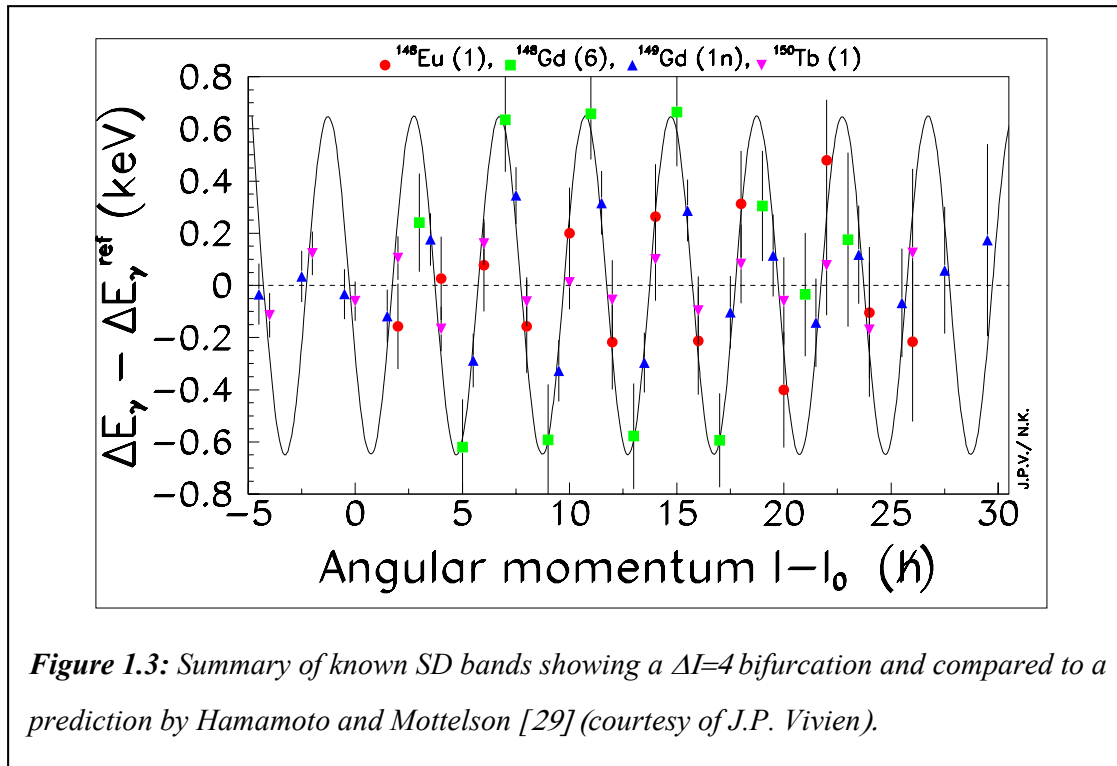
The search for new superdeformed rotational bands has revealed one of the most striking and unexpected results: the phenomenon of identical bands. It was first discovered in the nucleus  $^{151}\text{Tb}$  [15], for which the  $\gamma$ -ray transitions of the first excited superdeformed band were found to be within 2 keV of the transitions in the yrast superdeformed band of  $^{152}\text{Dy}$ . The associated dynamical moments of inertia  $\mathfrak{I}^{(2)}$  are then identical. The  $\mathfrak{I}^{(2)}$  moment depends on several contributions, like the mass, the deformation, the strength of the pairing field, the individual contribution

of each valence orbital etc.. Considering two neighbouring nuclei, differing by one neutron, the simplest way to explain identical dynamical moments of inertia is to assume some kind of cancellation effect between these contributions [23], but its origin is not yet fully understood.

In a typical fusion-evaporation experiment, many nuclei are produced and one could expect identical bands in several of those nuclei. In order to separate them, a high resolving power is needed. As illustrated in Figure 1.2, two almost identical superdeformed rotational bands belonging even to the same nucleus ( $^{143}\text{Eu}$ ) have been identified with EUROBALL [24]. From this result, the mass (or nucleon number) appears not to be a relevant degree of freedom in the description of

identical bands. For two superdeformed bands in  $^{194}\text{Hg}$  spins, parities and excitation energies have been established. Based on these results, a mechanism involving both pairing and particle alignment has been proposed to explain the identical band phenomenon [25]. In the  $A \sim 150$  mass region, on the other hand, where pairing correlations are supposed to be very weak, lifetime measurements indicate that alignment effects and deformation changes tend to compensate in identical bands [26]. A very similar phenomenon, called “shifted identical bands”, has been discovered more recently in deformed neutron-rich nuclei [27]. It appears that identical bands are probably not a unique property of the second well, but seem to indicate a more general aspect of nuclear structure.

### Staggering effects



The observation of  $\Delta I = 4$  bifurcation (also called  $\Delta I = 2$  staggering) in the yrast superdeformed band of  $^{149}\text{Gd}$  was another exciting development for nuclear structure studies. It has been suggested that staggering effects are due to the presence of a hexadecapole perturbation of the prolate superdeformed shape [16]. The  $\Delta I = 2$  rotational band is then split into two  $\Delta I = 4$  sequen-

ces, perturbed by about 120 eV relative to one another. This represents a tiny effect on the  $\gamma$ -ray energies which must be measured experimentally with a very high precision of about 0.1 keV. Thus, it is necessary to have a high-statistics spectrum of the superdeformed band without any contamination. This can only be achieved with a combination of very high resolving power and large efficiency. Up to now, staggering patterns, persisting over a large spin region, have been found in four superdeformed rotational bands using three different detectors EUROGAM, GAMMASPHERE and recently EUROBALL for  $^{150}\text{Tb}$  [28]. Hamamoto and Mottelson [29] have shown that, under some conditions, the magnitude of the staggering effects in two nuclei may be related. As shown in Figure 1.3, this theoretical interpretation fits well with the experimental data. In order to firmly establish the occurrence of such a staggering effect and to determine its microscopic origin the search for  $\Delta I = 4$  bifurcation must be extended to superdeformed nuclei in other mass regions.

### Coexistence of axial and triaxial superdeformed shapes

The possibility of prolate-triaxial shape coexistence in the second well has been highlighted by a EUROBALL experiment on  $^{154}\text{Er}$ . Several types of model calculations have predicted the lowest-lying superdeformed band in  $^{154}\text{Er}$  to be similar to the “doubly magic” yrast superdeformed band in  $^{152}\text{Dy}$ , which is based on the vacuum configuration in the pronounced prolate  $Z=66$ ,  $N=86$  shell gap. At  $Z=68$ , the additional two protons should occupy “spectator” orbits with low single-particle quadrupole moments. However, the first experimental observation of superdeformation in  $^{154}\text{Er}$  at GAMMASPHERE [30] revealed a superdeformed band with quite different characteristics. Primarily, the  $\mathfrak{I}^{(2)}$  moment of inertia for this band was significantly lower than the predictions. It was later suggested [31] that this superdeformed band might be the result of the nucleus having a triaxial shape. Recently, a second, weaker, superdeformed band was found in the analysis of EUROBALL data [20].

As can be seen in Figure 1.4 (b), the  $\mathfrak{I}^{(2)}$  moment of inertia of this band closely follows the predicted values for the lowest-lying prolate superdeformed band in  $^{154}\text{Er}$ , as well as the experimental values for the yrast superdeformed band in  $^{152}\text{Dy}$ . In the figure is also shown the  $\mathfrak{I}^{(2)}$  moment of inertia for the previously known band, together with the values predicted by Total Routhian Surface (TRS) calculations [20] for a triaxial superdeformed band. In Figure 1.4 (a) the  $\mathfrak{I}^{(1)}$

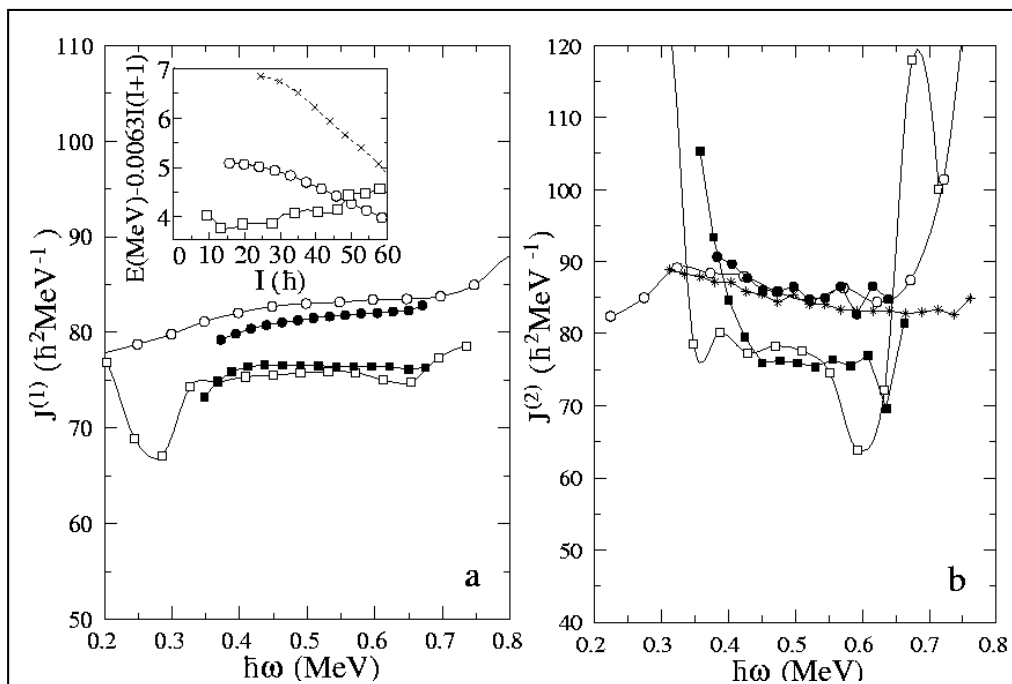


**Figure 1.4:** Moment of inertia plots for the two SD bands in  $^{154}\text{Er}$  as a function of rotational frequency: **(a)** kinematic moments  $\mathcal{J}^{(1)}$  and **(b)** dynamic moments  $\mathcal{J}^{(2)}$ . Open squares and open circles mark the theoretically predicted values for band 1 and 2, respectively, and filled squares and filled circles show the experimental values for bands 1 and 2. The inset shows theoretical excitation energies as a function of angular momentum for bands 1 and 2, as well as for the first excited prolate SD band (crosses). In the  $\mathcal{J}^{(2)}$  plot, the yrast superdeformed band in  $^{152}\text{Dy}$  (stars) is also included. The rise in the calculated  $\mathcal{J}^{(1)}$  moment of inertia at  $\hbar\omega \sim 0.65$  is due to rotational alignment of a pair of high- $j$  particles.

moments of inertia of the bands is compared to theoretical predictions. Here, a bandhead spin of  $24\hbar$  and  $26\hbar$  is assumed for the triaxial and prolate superdeformed bands, respectively. The inset of the figure shows theoretical excitation energies as a function of angular momentum for the lowest-lying and first excited prolate superdeformed bands, together with the predictions for the triaxial superdeformed band. The calculations not only agree with the rotational characteristics of the observed bands, but they are also consistent with the triaxial superdeformed band being more strongly populated than the prolate superdeformed band, i.e. in the angular momentum regime where the bands are fed in the experiment ( $45\text{--}55\hbar$ ) the prolate superdeformed band lies around 1 MeV higher than the other band.

### 1.3. Octupole softness and vibrations in superdeformed nuclei

In the  $A \sim 190$  mass region, octupole softness of the second well has been predicted by several theoretical models. This is illustrated in Figure 1.5 where the potential energy surface for  $^{194}\text{Pb}$  is plotted as a function of the quadrupole and octupole deformation parameters [32]. The second superdeformed well clearly appears to be much softer against the octupole degree of freedom than the first (spherical) well. Recent EUROBALL results have produced strong evidence that the lowest excited superdeformed states are, at least in some nuclei in the  $A \sim 190$  region, indeed based on octupole vibrational structures. To interpret the properties of excited superdeformed bands in  $^{197}\text{Pb}$  some octupole softness is needed in the quasi-particle description. These aspects will be discussed in more detail in the following sections.

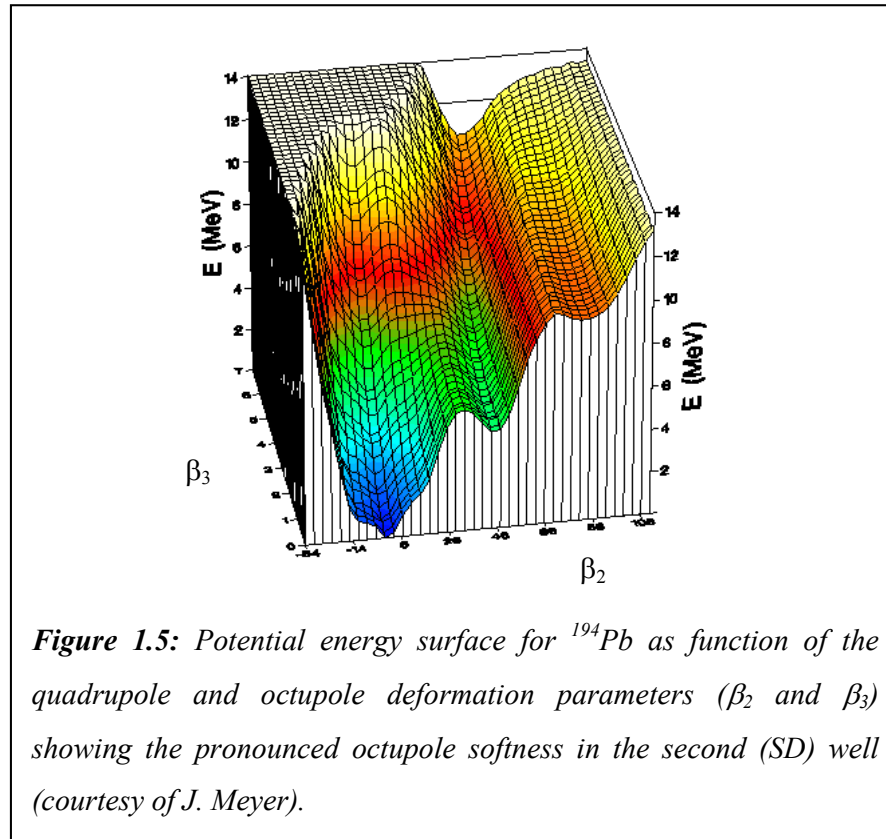
#### Octupole-vibrational superdeformed bands

Two EUROBALL experiments have been performed for  $^{190}\text{Hg}$  [33] and  $^{196}\text{Pb}$  [34,35] to establish the nature of  $\gamma$ -ray transitions connecting an excited superdeformed band with the yrast superdeformed band. In both cases, those transitions were intense enough to determine branching ratios for the inter-band and in-band decays, to measure angular distributions and to perform a linear polarisation analysis. Linear polarisation measurements are possible with EUROBALL since the Clover Ge detectors can be used as Compton polarimeters. The advantage of EUROBALL for this type of measurement is actually two fold: Firstly, clean (i.e. multi-gated) spectra can be obtained with sufficient statistics in the connecting transitions and secondly, the large detection efficiency of the Clover detectors allows the measurement of an accurate value of the polarisation. In the experiment on  $^{190}\text{Hg}$ , shown as an example in Figure 1.6,  $1.7 \cdot 10^9$  events were collected and about 12% of these were Compton-scattered events, which were used for the polarisation measurements.

Both experiments firmly establish the electric-dipole character of the inter-band transitions with a  $B(E1)$  strength of  $\sim 2 \cdot 10^{-3}$  Wu and  $\sim 10^{-4}$  W.u. for  $^{190}\text{Hg}$  and  $^{196}\text{Pb}$ , respectively. These values are much larger than the E1 transition strength observed between excited quasi-particle states, but they are similar to those found in normal-deformed nuclei, where octupole deformation (or vibration) is known to play an important role. To confirm this interpretation, lifetime measurements have been performed in  $^{196}\text{Pb}$  for both the yrast superdeformed band and the one based on the presumed



octupole vibration [34]. The quadrupole moments deduced for the two superdeformed bands agree within the experimental uncertainties. All these results provide strong evidence that at least some of the low-lying excited superdeformed bands in the  $A \sim 190$  mass region are of octupole-vibrational character.



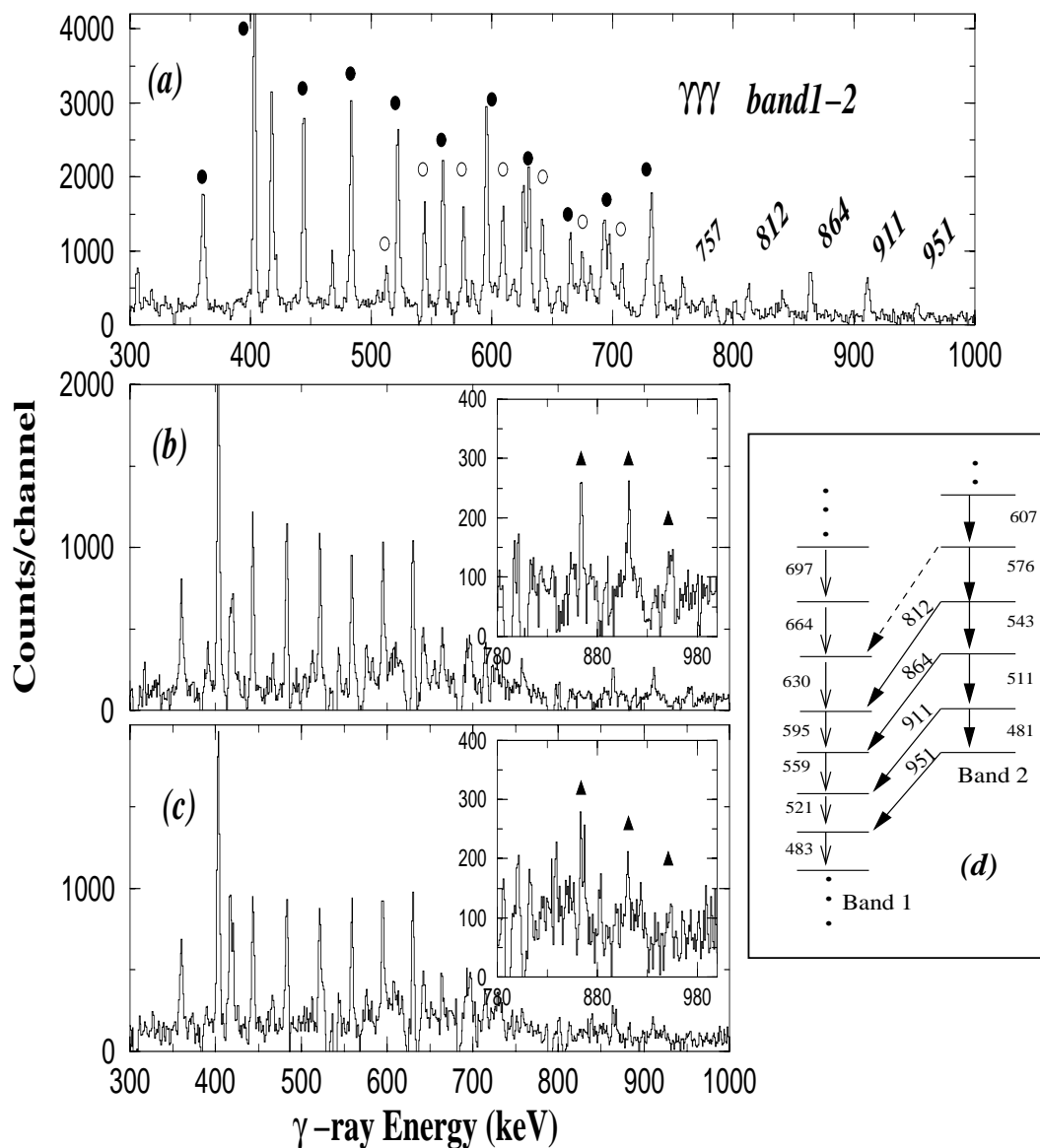


**Figure 1.6:** Spectroscopy of the superdeformed bands in  $^{190}\text{Hg}$ : Spectrum (a) shows transitions coincident with at least three  $\gamma$  rays from the first (○) or second (●) SD band. The transitions “linking” the two bands are labelled by their energies. Below spectra used for the linear polarisation analysis are shown, i.e. from  $\gamma$ -rays that were either vertically (b) or horizontally (c) scattered in the CLOVER detectors. The high energy portion of these spectra is detailed in the inset where the linking transitions are marked with triangles. Panel (d) shows the relevant portion of the level scheme [33].

**Influence of octupole softness in  $^{197}\text{Pb}$  and  $^{198}\text{Pb}$** 

In another recent EUROBALL experiment six new excited superdeformed rotational bands have been discovered in  $^{197-198}\text{Pb}$  [36]. The yrast superdeformed band in  $^{197}\text{Pb}$  ( $^{198}\text{Pb}$ ) represents only 0.2% (0.5%) of the corresponding reaction channel. This population is much weaker than in lighter lead nuclei and presumably related to the high excitation energy of the superdeformed states relative to the yrast line. Another difficulty in studying superdeformation in these heavy nuclei is the strong fission channel. Here, the INNER BALL calorimeter was decisive in order to reduce the strong fission background by selecting very long cascades. The new superdeformed bands have been interpreted in the framework of cranked HFB calculations with approximate projection on the particle number by means of the Lipkin-Nogami method [37]. In this way quasi-particle excitations have been assigned to all bands. However, in order to explain their rather large intensity (relative to the yrast superdeformed band), it was suggested that some excitations might be lowered in energy by the coupling with a residual octupole interaction of a non-axial  $Y_{32}$  type.

#### 1.4. Magnetic properties in the superdeformed minimum

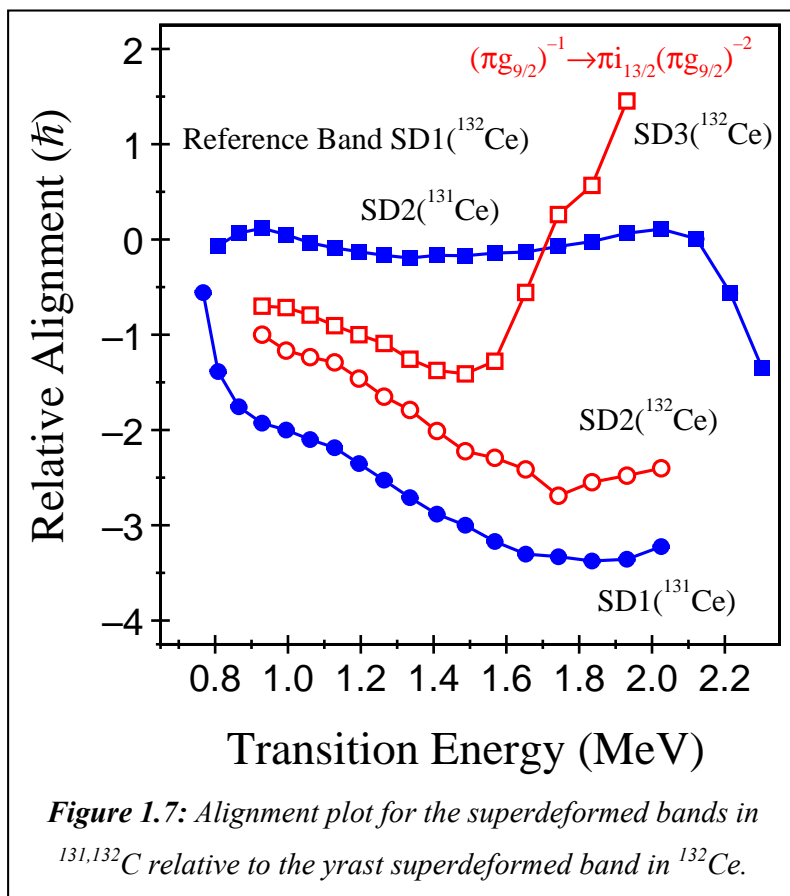
The EUROBALL data from the experiments described above also revealed the presence of “cross-talk” transitions between two superdeformed signature-partner bands in  $^{197}\text{Pb}$  [38]. Despite the very low intensities, i.e. the production cross section of the lowest excited superdeformed rotational band was estimated to  $\sim 0.5$  mb, directional correlations from oriented states (DCO) measurements were possible. The DCO ratios confirm the  $\Delta I=1$  character of the cross-talk transitions, but due to their low energy the (electric or magnetic) character could not be established from a measurement of their linear polarisation.

Assuming that the two bands are indeed signature partners, as indicated by the transition energies, the cross-talk transitions must have M1 multipolarity. Then  $B(M1)/B(E2)$  ratios can be determined experimentally for several states of the two bands. This ratio is proportional to  $(g_K - g_R) K / Q_0$ ,  $g_K$  and  $g_R$  being the single-particle and collective gyromagnetic ratio, respectively, and  $Q_0$  the intrinsic quadrupole moment. The collective  $g$ -factor can be estimated in the Inglis cranking approximation using microscopic HF+BCS calculations with the effective interaction SkM\* [39]. This approach is preferred since the  $g_R$  value found for superdeformed states can be different from the rigid-body  $Z/A$  estimate. Direct measurements of  $g$  factors in three superdeformed bands of  $^{194}\text{Hg}$  have confirmed the validity of this approach. If  $Q_0$  is known, for example from lifetime measurements, it is possible to experimentally determine the  $g_K$  value, which depends on the orbitals occupied by the valence particles. With this method precise quasi-particle configurations could be assigned to several superdeformed bands in nuclei around  $A \sim 190$  [22]. In addition, the effective spin-gyromagnetic factor  $g_s^{eff}$  can be derived from the  $g_K$  value, which appears to be close to the theoretical value for a free neutron ( $g_s^{free}$ ) indicating an unexpected lack of quenching for the neutron orbitals at superdeformed shapes [38]. More precise data on the  $B(M1)/B(E2)$  ratios are still needed to fully understand the underlying reasons for this apparent lack of quenching.

### 1.5. Structure of superdeformed bands in $^{131,132}\text{Ce}$

The two superdeformed bands in  $^{131}\text{Ce}$  and the three superdeformed bands in  $^{132}\text{Ce}$  have been extended to higher spin with recent EUROBALL IV data. While none of the five bands have been connected into the normally deformed states, the two bands in  $^{131}\text{Ce}$  have been linked to each other by three transitions. Angular correlation results indicate a  $\Delta I=1$  M1/E2 character with a substantial E2/M1 mixing ratio ( $\delta \sim +1$ ). It has also been possible, for the first time, to measure angular correlation ratios for the in-band transitions in all five SD bands.

The relative alignments of the SD bands are shown in Figure 1.7, with the yrast SD1 band of  $^{132}\text{Ce}$  used as reference. The



important ingredient of the latter band is the  $(\pi g_{9/2})^{-2}(v i_{13/2})^2$  configuration. The excited SD2 band in  $^{131}\text{Ce}$  (with zero relative alignment) must also involve this structure, while the yrast SD1 band in  $^{131}\text{Ce}$  (with less alignment) loses one of the  $i_{13/2}$  neutrons. The excited SD2 and SD3 bands in  $^{132}\text{Ce}$  are interpreted in terms of signature partner bands built on the  $(\pi g_{9/2})^{-1}(v i_{13/2})^2$  configuration (cf. the SD bands in  $^{133}\text{Pr}$  [40]). It can be seen that SD3 gains alignment above a transition energy of 1.6 MeV (i.e.,  $\omega \sim 0.8$  MeV/h) which is attributed to a crossing between the high- $\Omega$   $\pi g_{9/2}$  orbital and the first low- $\Omega$   $\pi i_{13/2}$  intruder orbital. The structure of SD3 at high spin is then  $(\pi g_{9/2})^{-2}(\pi i_{13/2})^1(v i_{13/2})^2$ . This crossing provides the first evidence for the  $i_{13/2}$  proton intruder in the cerium nuclei ( $Z=58$ ); this orbital is usually only observed in superdeformed structures in nuclei with  $Z \geq 63$ .

## 1.6. Search for Hyperdeformation

One of the main goals of nuclear structure research has been to observe hyperdeformed (HD) nuclear states at extremes of angular momentum. Such states are theoretically predicted in various regions of the nuclear chart and will become yrast at very high values of spin, typically above  $80\hbar$  [41-, 42, 43, 44, 45]. These states have very large prolate deformations with major to minor axis ratios of approximately 3:1. The discovery of hyperdeformed states at high angular momentum would be a very important test of nuclear models, and therefore the search for hyperdeformed states was an important part of the justification for constructing the EUROBALL array.

Many searches have been carried out for signals of HD nuclear shapes [46-, 47, 48, 49, 50, 51], however, as yet no compelling evidence for the existence of discrete hyperdeformed states at high spin exists. One of these searches has been performed in one of the first experiments with EUROBALL [52]. But many searches have been carried out without any prior experimental information about how much angular momentum these candidate nuclei can support before undergoing fission. Therefore, the non-observation of these states may be a direct consequence of fission or high evaporated-particle multiplicities imposing a limit on the angular momentum in the residual nucleus of study.

At such extremes of angular momentum and deformation it is not clear what parameterisations will allow the prediction of the correct sequence of single particle levels to create the shell gaps necessary to stabilize these deformations. Therefore, it may also be possible that hyperdeformed states have not yet been observed because of the failure of current models under such extremes of spin, and these models are predicting hyperdeformed minima to occur in the wrong nuclei.

### Candidate nuclei

It is also interesting to note that gamma-ray spectra of superdeformed bands obtained with the latest generation of spectrometers (EUROBALL and GAMMASPHERE) only show, at best, 2-3 new transitions (on top of previously known bands), despite the spectra having 2-3 orders of magnitude more counts, and the arrays having two orders of magnitude better resolving power than the previous generation. This implies that something other than advances in detector technology is placing a limit on the ability to study states at the extremes of nuclear spin. We suggest this limit is

primarily due to fission and/or excessive particle evaporation, and that too little attention has been paid to the reaction and reaction conditions necessary to populate HD states. Therefore, the system to be studied must be chosen very carefully. From recent experiments the following criteria for choosing the reaction to be studied could be extracted:

- 1) Compound nuclei must be in the mass  $A \sim 100-170$  range, since this is the only region in which fission limits may be high enough to allow the population of very high spin states [53].
- 2) Since the fissility of the compound system increases with  $Z^2/A$ , the isotope under study must be as neutron rich as possible for a given element. In fact, intense neutron-rich radioactive ion beams are the best choice in order to maximise the angular momentum input into the compound nucleus.
- 3) Symmetric reactions are highly preferable since their Q-values are usually much lower than those of asymmetric ones allowing colder formation of the compound system. Furthermore, some experiments show that high spin states are more strongly favoured with such reactions (e.g the superdeformed band in  $^{148}\text{Gd}$  is enhanced 4.6 times with symmetric reactions rather than asymmetric ones [54]). Neutron multiplicities will also be lower, therefore less angular momentum will be removed from the compound system.
- 4) Reactions involving beam/target combinations which are near magic, magic or doubly magic are also desirable, since the shell effects lower the Q-value of the reaction (e.g. when populating heavy elements [55] magic beam-target combinations are essential for these nuclei to be produced with as little fission as possible).
- 5) Suggestions have also been made [47,48] that detection of a proton in coincidence with gamma rays may enhance the probability of observing hyperdeformed structures. This may help for two reasons: Firstly, the peak to background ratio improves considerably because unwanted reaction channels and fission are rejected. Secondly, emission of protons from the hyperdeformed compound system might be enhanced due a lower Coulomb barrier at the “tips” of an extremely deformed shape where the charge is concentrating.

- 6) Exit channels with the lowest number of particles emitted have the best chance of being populated at the highest spins necessary to populate hyperdeformed shapes. Of particular interest are reaction channels such as  $2n$ ,  $3n$  or  $p2n$ . These can be enhanced using the high-fold data from the inner BGO ball, and/or techniques such as  $\gamma$ -ray filtering [56].

Hyperdeformed minima are predicted in a wide range of nuclei between masses 130 and 170 [41-45]. It is interesting to note that in previous studies of rotational bands based on superdeformed shapes, the occurrence of second minima in the nuclear potential energy is a widespread phenomenon. Since many more energy levels intrude and cross over from shells above at even higher deformations it is expected that hyperdeformed shell gaps will be even more abundant than superdeformed shell gaps. What is not clear is whether it is possible to generate sufficient angular momentum, without inducing fission, to populate these minima in any of the nuclei accessible with stable beams and targets in this region. Furthermore, it is not clear how low in spin these minima persist. For long rotational superdeformed bands it has been observed empirically that it is possible to study structures as weak as  $10^{-5}$  of a reaction channel. Provided that a hyperdeformed cascade is long (greater than 5 transitions), this observationally limit can be reached. However, the resolving power of EUROBALL may still not be sufficient for observation of such structures.

### Recent EUROBALL Experiments

Four experiments fulfilling the criteria suggested in the introduction have been performed with the EUROBALL array, the latest being a very long experiment of  $\sim 4$  weeks of beam time.

The reactions studied/to be studied are:

- (i)  $^{48}\text{Ca} + ^{82}\text{Se}$  (June 2001 – Euroball)
- (ii)  $^{50}\text{Ti} + ^{124}\text{Sn}$  (June 2001 – Euroball)
- (iii)  $^{48}\text{Ca} + ^{96}\text{Zr}$  (June 2002 – Euroball)
- (iv)  $^{64}\text{Ni} + ^{64}\text{Ni}$  (January 2002 & December 2002 – EUROBALL + DIAMANT)



The most promising results so far have come from the  $^{48}\text{Ca} + ^{82}\text{Se}$  experiment producing isotopes of Xe. A candidate rotational structure with approximately 10 very weak evenly spaced transitions ( $\Delta E_\gamma \sim 33$  keV) was found, however, the statistical significance of this structure ( $\sigma = 2.31$ ) was not sufficient to confirm that the sequence was real and not a statistical aberration. Extensive work on analysis of these data is ongoing.

### **Future perspectives**

EUROBALL, together with its counterpart GAMMASPHERE, has provided many new results on the superdeformed world of nuclei. But these results also show that many experiments are on the very limits of what can be done with present arrays. This is especially true for more information on spins, parities and excitation energies of superdeformed states and for the search for hyperdeformed nuclei. New data in these domains can only be provided by a new generation of  $\gamma$ -ray spectrometers built from  $\gamma$ -ray tracking detectors with a much increased efficiency and resolving power.

### **Acknowledgements**

The reported work stems from a large collaboration within the EUROBALL users community. In particular, the authors like to acknowledge A. Astier, A. Axelsson, N. Buforn, B. Herskind, H. Hübel, A. Korichi, K. Lagergren, M. Meyer, B. Nyako, E. Paul, M.-G. Porquet, N. Redon, D. Rossbach, and J.-P. Vivien for having us provided their results and for fruitful discussions.